Perampalam Gatheeshgar
Keerthan Poologanathan*
Shanmuganathan Gunalan
Brabha Nagaratnam
Konstantinos Daniel Tsavdaridis
Jun Ye

Structural behaviour of optimised cold-formed steel beams

Cold-formed steel (CFS) members have been significantly employed in light gauge steel buildings due to their inherent advantages. Optimising these CFS members in order to gain enhanced load bearing capacity will result in economical and efficient building solutions. This research presents the investigation on the optimisation of CFS members subjected to flexural capacity and results. The optimisation procedure was performed using Particle Swarm Optimisation (PSO) method while the section moment capacity was determined based on the effective width method adopted in EN1993-1-3 (EC3). Theoretical and manufacturing constraints were incorporated while optimising the CFS cross-sections. In total, four CFS sections (Lipped Channel Beam (LCB), Optimised LCB, Folded-Flange and Super-Sigma) were considered including novel sections in the optimisation process. The section moment capacities of these sections were also obtained through non-linear Finite Element (FE) analysis and compared with the EC3 based optimised section moment capacities. Results show that compared to the commercially available LCB with the same amount of material, the novel CFS sections possess the highest section moment capacity enhancements up to 65%. In addition, the performance of these CFS sections subject to shear and web crippling actions were also investigated using non-linear FE analysis.

1 Introduction

CFS structural members sustain their position in the light gauge construction industry. This is due to the significant advantages of CFS including high strength to weight ratio, easy to transport, able to employ all conventional jointing methods, cost effective, high quality control, dimensional stability and flexibility in manufacturing profiles over hot-rolled sections. These advantages led the extensive use of CFS members in low-to mid-rise buildings and modular buildings. Conventional C, Z and hat CFS sections are commonly employed as flexural members in construction framework [1, 2]. The thin-walled nature of CFS is deemed to have local, distortional and global buckling instabilities even at a stress level below yield strength. To minimise the buckling instabilities by eliminating the free edges, hollow flange sections were developed and subjected to extensive research studies [3-6] to investigate their various structural behaviours of bending, shear and web crippling actions. The development of the Direct Strength Method (DSM) raised a subject of innovative and complex section profiles of CFS members [7]. In addition, advanced Finite Element (FE) software packages have made a path to examine innovative CFS sections in detail. These innovative and complex sections can be manufactured through advanced manufacturing technologies. Moreover, these sophisticated technologies offer the measurement of mechanical properties of CFS through non-destructive testing methods. Generally, the main mechanical parameters of CFS such as yield strength and tensile strength are measured from destructive tensile tests (tensile coupon tests). Nowadays, non-destructive 3MA techniques are successfully employed to determine the unknown material characteristics of yield,

tensile strength as well as the residual stress distribution [8-10]. This leads to focus more towards optimisation framework even though that results in complex sections because the difficulty in determining the mechanical properties of CFS members can be achieved via non-destructive testing methods.

The optimisation process is essential to enhance the structural performance of the building and to ensure lightweight structures. To date, several optimisation methods have been adopted including the neural network [11], genetic algorithm [12-14] and trust region method [15] to optimise the CFS beams for different criteria. Recently, Particle Swarm Optimisation (PSO) was used to optimise the bending capacity of CFS lipped channel beams (LCB) with intermediate and edge stiffeners, and an innovative folded-flange beam [16, 17]. It was noticed that the aforementioned studies were not assessed their performance under shear and web crippling actions and no optimisation works were carried out for sigma sections.

This paper aims to introduce novel CFS beam sections which have enhanced flexural capacity along with minimal torsional effect. In addition, their corresponding behaviour under shear and web crippling actions were also investigated through FE analysis. To emphasise the structural benefits of the considered sections, bending, shear and web crippling capacities were compared with a commercially available LCB section with the same amount of material.

2 Optimisation of cold-formed steel sections

This section provides detail on the optimisation process. Four CFS prototypes were considered for the optimisation as shown in Fig. 1. During the optimisation, the amount of material (Coil length = 415 mm and thickness = 1.5 mm) was maintained constant to evaluate the structural performance of the novel sections over a commercially available benchmark section (see Fig. 1a). Further, the modulus of elasticity, Poisson's ratio and yield stress were considered as 210 000 MPa, 0.3 and 450 MPa, respectively.

Optimisation studies employing advanced algorithms are recently seen more often to improve the design and performance of structural elements and systems [18-22]. In this study, PSO was employed for the optimisation of CFS sections. PSO has similarities with the Genetic Algorithm (GA) as they both are based on populations. PSO, however, claims more recognition than GA because of the computationally efficient nature [23]. The solutions, termed particles (N), are treated as points within the problem space. The optimisation process is initiated by creating positions of particles and assigning them initial velocities. Each particle evaluates the objective function with respect to its position and updates the best function value and the best (optimum) location. During the iteration, particles tend to change their position by updating the velocity using the available information of current velocity, the particles individual best positions, and best locations of their neighbourhood mates. The comprehensive detail on PSO can be found elsewhere [16, 17].

The aim of using the PSO tool is to maximise the section moment capacity of CFS prototypes. Therefore, the optimisation problem can be expressed as:

$$M_{c,Rd} = [W_{eff}(x)]_{max} \cdot f_y \quad d_{min} \leq x_i \leq d_{max} \quad for\ i = 1, 2, .., N \tag{3}$$

Where $M_{c,Rd}$ is the moment resisting capacity of the cross-section and $W_{eff}(x)$ is the effective section modulus about major axis bending. The section moment capacity is calculated according to the effective width method adopted in EN1993-1-3 (EC3) [24]. The theoretical constraints defined in EC3 and manufacturing limitations for the segments of the prototype sections are set as lower bound, d_{min} and upper bound, d_{max}. The aforementioned design and optimisation processes were executed with Matlab [25]. Similarly, effective with method based section moment capacity calculations adopted in AS/NZ 4600 [26] and AISI S100 [27], and corresponding steel grades can also be used to develop the optimisation problem. The optimised dimensions of the considered novel prototypes are provided in Table 1.

The torsional effect in CFS members is highly governed by transverse eccentric loading. In general practice, CFS beam sections are often loaded eccentrically, commonly through the flange and few occasions through the web, for example, beam-beam connections (in floor panels and mezzanine floor systems). Hence, the failure type is combined bending and torsion, not pure bending failure [28]. Gotluru et al. [29] claimed that due to the open nature of the sections, the developed torque due to the eccentric loading also induces warping in the beam and concluded that the ultimate state is meaningless compared to the serviceability limit state, due to the large rotation of the beams before failure. It is apparent that additional restraints are required to avoid torsional action. Moreover, the optimisation was performed with respect to the loads and have not taken into account practical connection details [30] that may change the load path. Super-Sigma section has an additional benefit of the closer shear centre to the web thus minimises the twisting action. Therefore, this alleviates the need for additional torsional restraints.

3 Numerical modelling

3.1 General

This section provides the description of the material and geometrical non-linear FE modelling and analysis to investigate the flexure, shear and web crippling behaviour of selected CFS prototypes. The FE software package ABAQUS version 2017 [31] was employed for the analysis. All FE models were developed as perfect plasticity models with nominal yield stress due to the negligible strain hardening nature of CFS [32], while the magnitude of the geometrical imperfection was considered as a function of the clear web height ($0.006d_1$) as proposed in [33]. This magnitude was incorporated into the nonlinear analysis through *IMPERFECTION command and performing buckling analysis. Thus two methods of analysis were performed: (a) Eigenvalue buckling analysis to incorporate the geometrical imperfection magnitude, and (b) Non-linear static analysis to include the large deformations and material yielding effects.

All prototype sections were created using three-dimensional S4R shell elements which have the ability of reduced integrations and less computation time. A uniform mesh size of 5 mm × 5 mm was used for the webs and flanges except for the corner regions. Since the corner regions are critical, therefore, 1 mm × 5 mm mesh size was assigned. The load and boundary conditions were provided through the Web Side Plates (WSPs) which are attached to the model. The WSPs were also constructed using S4R shell elements, however, 10 mm × 10 mm mesh size was used as they do not influence the prototype's behaviour. Moreover, WSPs for the Super-Sigma sections were simulated with coupling constraints as it has intermediate web stiffener and difficult to attach web plates. A detailed description of Flexural, shear and web crippling model development is presented, followed by its verification against experimental data.

3.2 Flexural behaviour

The flexural behaviour of CFS sections was analysed by developing a four-point loading test model (middle and two adjacent spans of 500 mm and 1500 mm, respectively) as it ensures the pure bending failure in the mid-span with the absence of shear force in that region. Simply supported boundary conditions were implemented and displacement control loading at the shear centre approach was performed for all prototypes. These were achieved by attaching full height WSPs using 'tie' constrain option available in ABAQUS. Straps were simulated as boundary conditions in 250 mm intervals at the top and bottom flanges in order to simulate the floor joist and roof purlin as in real-world application where toppings are inevitable, for example, roof sheathing and concrete toppings. It is noteworthy to mention that non-linear static analysis was performed for bending. The extensive detailed work presented in [34-36] was followed to develop and analyse the flexural behaviour of CFS channels.

The failure modes obtained for the Folded-Flange section at different stages are depicted in Fig. 2. The

ultimate bending capacities obtained from the FE analysis for the prototypes are verified against EC3 (see Table 1)

3.3 Shear Behaviour

This section investigates the shear behaviour of the novel sections with the aid of FE analysis. Several key parameters should be decided such as the aspect ratios, mainly, the ratio between shear span and clear web height to achieve pure shear failure. Relatively short span (aspect ratio = 1.0) three-point loading arrangement was selected to construct the FE model which ensures the pure shear failure due to the presence of the negligible flexural moment. Simply supported boundary conditions were provided to the model. The extensive detail on finite element modelling of CFS beams subject to shear was followed from previous research work [37-39]. Fig. 3 shows the deformation failure mode obtained through FE analysis for Super-Sigma sections at different stages. Straps were simulated as boundary conditions at the flanges in corresponding edge points of WSPs. These straps were provided to cater the flange distortion due to unbalanced shear flow nature in open CFS sections when subject to shear loading. Similar to the bending model, shear center loading was performed with the aid of WSPs and these WSPs were connected to the model using 'tie' constraint. The WSPs were simulated with coupling constraints for Super-Sigma sections as elaborated in section 3.1. It is noteworthy to mention that non-linear static analysis was performed as similar to the bending model.

3.4 Web crippling behaviour

Web crippling is one of the special local and global failure modes of thin-walled CFS sections when subjected to concentrated loads. In this study, all considered innovative optimised CFS prototypes were also evaluated under the web crippling failure. Even though four types of web crippling load cases are present, this study focuses on the interior two flanges (ITF) load case only. In order to develop the FE models for the ITF load case, the extensive detailed work presented in [40] was followed and the brief details used to construct the models are described in this section.

For web crippling models, loading plates were constructed using R3D4 discrete rigid plate elements. The web crippling capacity is highly sensitive to the bending radius of the corners which governs the plastic deformation of the web-flange junction. Therefore, finer mesh refinement was accommodated to those critical regions. The extruding length of the model was taken as $5d_1$, where d_1 is the clear web height of the prototype section, which is also acknowledged in Sundararajah et al. [41]. The width of the loading and supporting plates used was 100 mm. Simply supported boundary conditions (pin supports) were assigned to the reference point of the loading and bearing plates, while only the loading plate is allowed to translate vertically downwards by displacement control approach. The effect of the geometric imperfections was not considered in the model due to its negligible influence (less than 1%) in the web crippling capacity as reported in [40]. Moreover, surface-to-surface contact option in ABAQUS was assigned between the bearing and loading plates and the primary model, and the friction coefficient between these two was set to be 0.4. Contact formulation was chosen to be 'hard' contact available in ABAQUS. The analysis of this web crippling models was run using the quasi-static analytical option in order to avoid the contact difficulties in the non-linear static approach. The failure modes obtained in different stages for the Optimised LCB section through FE analysis is illustrated Fig 4.

Section 3.2, 3.3 and 3.4 elaborated about the FE model development of the considered innovative optimised sections subject to bending, shear, and web crippling actions, respectively. Fig. 5 depicts the load-displacement behaviour obtained for all considered CFS sections obtained through FE analysis.

3.5 Validation of finite element models

All the aforementioned model characteristics for bending, shear and web crippling actions were validated

with the experimental results obtained by Pham and Hancock [2], Keerthan and Mahendran [42] and Sundararaja et al. [41], respectively. The four-point loading set-up used in Pham and Hancock's [2] study is showed in Fig. 6a to account local and distortional buckling failures. The bending results provided in Table 2 are the ultimate bending capacities for LCB sections which allowed to fail under distortional buckling by providing straps at top and bottom flange loading points and supports. The FE results showed a good agreement with the experiments with a mean of 0.97 and COV 0.07 for 6 bending test specimens. Keerthan and Mahendran [42] performed pure shear test of LCB sections with simply supported three-point loading arrangement. Back-to-back test arrangement (see Fig. 6b) was used to avoid the eccentric loading of shear centre and straps were used at top and bottom flanges at loading and supporting points to cater the flange distortion due to the unbalanced shear flow. The comparison of 6 test results with FE ultimate shear capacities for LCB sections which allowed to fail under pure shear with an aspect ratio of 1.0 is given in Table 3. FE results revealed a good agreement with the experimental results with a mean of 0.99 and COV 0.08. Sundararaja et al. [41] investigated the structural behaviour of LCB sections subject to ITF load case web crippling actions and in more advance several research studies on web crippling behaviour of European grade CFS beams with web openings [43-50]. The schematic diagram and web crippling test set-up used for ITF load case is shown in Fig. 6c. The ultimate web crippling capacities of the 6 test specimens and the FE results are presented in Table 4. The FE results revealed an excellent agreement with the experimental results with a mean and a COV of 0.99 and 0.02, respectively. Fig. 7 depicts the comparison of failure modes and load-vertical displacement behaviour obtained through validation. For the shear and web crippling, even though FE models reach the ultimate capacity with lesser displacement, their ultimate capacities show satisfactory agreement with test capacity. The aforementioned variation may due to the common initial bolt slip occur in experiments and it is hard to simulate this phenomena in FE modelling. These comparisons further confirm the accuracy of the developed FE models to predict the ultimate capacity and failure modes of considered CFS sections for bending, shear and web crippling actions.

4 Results and Discussion

This study presents the optimised innovative CFS beam sections for flexural capacity and the structural performance of the optimised innovative sections subject to shear and web crippling actions. The results obtained for the considered CFS sections from the EC3 and FE analysis are compared with a commercially available benchmark LCB section to evaluate the performance. The overall results of the FE analysis conducted for bending, shear and web crippling actions using a general purpose FE software package ABAQUS are demonstrated in Table 5.

The bending capacities of the sections are compared by setting the ultimate bending capacity of the benchmark LCB section obtained from FE to 100%. Super-Sigma section is the efficient section in bending as it bears approximately 65% of higher capacity than the benchmark section with same amount of material. Moreover, the Folded-Flange section claims about 60% of flexural capacity enhancement. It is noticed that when the available LCB section subjects to optimisation, it resulted in nearly 30% of the flexural capacity enhancement. These findings reveal the available LCB sections which are mostly used in light gauge steel construction as floor joists and purlins (flexural members) can be used in an effective way with the same amount of material. Thus provides the most economical and efficient design solutions. In addition, commonly sigma section used as purlins to date and rare usage has been noticed as floor joists. It is proposed that Super-Sigma sections can be employed as a flexural member in floor panels instead of conventional LCB section as it has enhanced flexural capacity, moreover, closer shear centre to the outer web which contributes to minimise the eccentric loading.

The optimised innovative sections, when subject to shear actions, behave in a positive way in terms of structural capacity over available benchmark section except for the folded-flange section. The Optimised

LCB and Super-Sigma section show 1% and 16% of shear capacity enhancement while Folded-Flange section experiences a considerable 26% of shear capacity reduction as provided in Table 5. Therefore, further modification on the shape and size are required to avoid this shear capacity reduction. Similarly, the web crippling capacity of the optimised sections also registers a web crippling capacity loss over benchmark LCB section with same amount of material. The optimised LCB and Super-Sigma sections claim 12% and 17% of web crippling capacity loss, respectively. However, Folded-Flange section experiences a substantial amount of web crippling capacity reduction of about 40%. It is worth to note that further modification on this innovative CFS sections are necessary to improve the web crippling capacity. The common practice is attaching rigid web plates at loading points.

The proposed optimised sections have excellent characteristics in terms of enhanced flexural capacity. Super-Sigma section owns highest bending capacity enhancement among the considered CFS sections and its intermediate web stiffeners bring back the shear centre closer to the outer web thus minimises the torsional effects under eccentric loading. This is an additional benefit of the Super-Sigma section. As a result, this research outcome would drive sigma sections to employ extensively in light gauge steel and modular building construction as load-bearing purlins, floor joist, and side rails. The general design method for thin-walled CFS beams is based on elastic theory, for example, effective with methods and direct strength methods. It should be noted that these methods are well established for LCB sections subjected to bending shear and web crippling actions and not for Folded-Flange and Super-Sigma sections. Therefore, further research needs to focus on creating a wide range of data set through physical testing and FE modelling and searching for modifications to improve for enhancing the web crippling and shear capacity. This would increase the use of these optimised novel sections. It is envisioned that incorporation of these optimised sections in construction will significantly reduce the entire structures' weight. Therefore, the proposed novel sections including super-sigma sections are suitable for floor joist and roof purlin applications as well as for modular building applications.

5 Concluding remarks

This research presents the optimisation framework of CFS members to maximize flexural capacity through EC3 and PSO. In addition, the performance of the innovative optimised sections subject to shear and web crippling action were also investigated using FE analysis. It was found that for the same amount of material, Folded-Flange and Super-Sigma sections have a higher flexural capacity enhancement of approximately 60% and 65%, respectively. The Super-Sigma section was found to be an efficient section investigating its overall performance under bending, shear and web crippling actions. Therefore, the Super-Sigma section is proposed to employ as floor/roof joists or purlins in light gauge steel construction as it claims substantial enhancement in flexural capacity and closer shear centre to the web thus minimises the torsional effect due to the eccentric loading. However, the behaviour of novel optimised CFS members after linear-response may not be predicted accurately through FE due to the new shapes and folding configurations. Thus, the predicted deflections may not be accurate, though the predicted the ultimate capacities from FE analysis are reasonably accurate. Considering this, further research is in progress to perform a series of structural tests for the optimised innovative sections for bending, shear and web crippling actions and developing new design equations.

Acknowledgements

The authors would like to express their gratitude towards Northumbria University and MMCEngineer Ltd for providing the financial support and the necessary facilities to conduct this research project.

References

[1] Laím, L., Rodrigues, J., Craveiro, C.: Flexural behaviour of beams made of cold-formed steel sigma-shaped sections at ambient and fire conditions, *Thin-Walled Structures*. 87 (2015), pp. 53-65.

[2] Pham, C., Hancock, G.: Experimental Investigation and Direct Strength Design of High-Strength, Complex C-Sections in Pure Bending, *Journal of Structural Engineering*. 139 (2013), pp. 1842-1852.

[3] Keerthan, P., Mahendran, M.: Experimental studies on the shear behaviour and strength of LiteSteel beams, *Engineering Structures*. 32 (2010), pp. 3235-3247.

[4] Keerthan, P., Mahendran, M.: Improved shear design rules of cold-formed steel beams, *Engineering Structures*. 99 (2015), pp. 603-615.

[5] Steau, E., Keerthan, P., Mahendran, M.: Web crippling capacities of rivet fastened rectangular hollow flange channel beams under one flange load cases, *Steel Construction*. 9 (2016), pp. 222-239.

[6] Siahaan, R., Mahendran, M., Keerthan, P.: Section moment capacity tests of rivet fastened rectangular hollow flange channel beams, *Journal Of Constructional Steel Research*. 125 (2016), pp. 252-262.

[7] Schafer, B.: Cold-formed steel structures around the world, *Steel Construction*. 4 (2011), pp. 141-149.

[8] Wolter, B., Gabi, Y., Conrad, C.: Nondestructive Testing with 3MA—An Overview of Principles and Applications, *Applied Sciences*. 9 (2019), pp. 1068.

[9] Fox, C., Doktor, D., Kurz, W., Seiler, G., Wu, H., Boller, C.: Evaluation of steel buildings by means of non-destructive testing methods, *Ce/Papers*. 1 (2017), pp. 4560-4569.

[10] Doktor, M., Fox, C., Kurz, W., Stockis, J.: Characterization of steel buildings by means of non-destructive testing methods, *Journal of Mathematics In Industry*. 8 (2018).

[11] Adeli, H., Karim, A.: Neural Network Model for Optimization of Cold-Formed Steel Beams, *Journal of Structural Engineering*. 123 (1997), pp. 1535-1543.

[12] Lee, J., Kim, S., Park, H., Woo, B.: Optimum design of cold-formed steel channel beams using micro Genetic Algorithm, *Engineering Structures*. 27 (2005), pp. 17-24.

[13] Magnucki, K., Maćkiewicz, M., Lewiński, J.: Optimal design of a mono-symmetrical open cross section of a cold-formed beam with cosinusoidally corrugated flanges, *Thin-Walled Structures*. 44 (2006), pp. 554-562.

[14] Magnucki, K, Rodak, M., Lewiński, J.: Optimization of mono- and anti-symmetrical I-sections of cold-formed thin-walled beams, *Thin-Walled Structures*. 44 (2006), pp. 832-836.

[15] Tran, T., Li, L.: Global optimization of cold-formed steel channel sections, *Thin-Walled Structures*. 44 (2006), pp. 399-406.

[16] Ye, J., Hajirasouliha, I., Becque, J., Eslami, A.: Optimum design of cold-formed steel beams using Particle Swarm Optimisation method, *Journal Of Constructional Steel Research*. 122 (2016), pp. 80-93.

[17] Ye, J., Hajirasouliha, I., Becque, J., Pilakoutas, K.: Development of more efficient cold-formed steel channel sections in bending, *Thin-Walled Structures*. 101 (2016), pp. 1-13.

[18] Grekavicius, L., Hughes, J., Tsavdaridis, K., Efthymiou, E.: Novel Morphologies of Aluminium Cross-Sections through Structural Topology Optimization Techniques, *Key Engineering Materials*. 710 (2016), pp.321-326.

[19] Tsavdaridis, K., Kingman, J., Toropov, V.: Application of structural topology optimisation to perforated steel beams, *Computers & Structures*. 158 (2015), pp. 108-123.

[20] Tsavdaridis, K.:Applications of Topology Optimization in Structural Engineering: High - Rise Buildings and Steel Components, *Jordan Journal Of Civil Engineering*. 9 (2015), pp. 335-357.

[21] Tsavdaridis, K., D'Mello, C.: Optimisation of novel elliptically-based web opening shapes of perforated steel beams, *Journal Of Constructional Steel Research*. 76 (2012), pp. 39-53.

[22] Tsavdaridis, K. D., D'Mello, C.: Finite element investigation of perforated beams with different web opening configurations, in: *The 6th International Conference on Advances is Steel Structures* (ICASS 2009). 16-18 December 2009, Hong Kong, China, pp. 213-220.

[23] Hassan, R., Cohanim, B., De Weck, O.: A comparison of particle swarm optimisation and genetic algorithm, in: *1St AIAA Multidisciplinary Design Optimization Specialist Conference*, 2005: pp. 18-21.

[24] CEN, Eurocode3: Design of Steel Structures, Part1.3: General Rules - Supplementary Rules for Cold-formed Steel Members and Sheeting, in, Brussels: European Committee for Standardization, 2005.

[25] Mathworks, Matlab R2017a, in, Mathworks, Inc, 2017.

[26] Standards Australia, AS/NZS 4600:2018: Cold-formed steel structures. Sydney, Australia, 2005.

[27] American Iron and Steel Institute (AISI), Specifications for the cold-formed steel structural members, cold-formed steel design manual, AISI S100, Washington DC, USA, 2016.

[28] Bogdan, M., Young -Lin, P., Trahair, N. S.: Bending and Torsion of Cold-Formed Channel Beams, *Journal of Structural Engineering*. 125 (1999), pp. 540-546.

[29] Gotluru, B., Schafer, B., Peköz, T.: Torsion in thin-walled cold-formed steel beams, *Thin-Walled Structures*. 37 (2000), pp. 127-145.

[30] Lim, J., Hancock, G., Charles Clifton, G., Pham, C., Das, R.: DSM for ultimate strength of bolted moment-connections between cold-formed steel channel members, *Journal Of Constructional Steel Research*. 117 (2016), pp. 196-203.

[31] ABAQUS, in, Hibbitt, Karlsson & Sorensen, Inc, Pawtucket, USA, 2007

[32] Keerthan, P., Mahendran, M.: New design rules for the shear strength of Lite Steel beams, *Journal of Constructional Steel Research*. 67 (2011), pp. 1050-1063.

[33] Schafer, B., Peköz, T.: Computational modelling of cold-formed steel: characterizing geometric imperfections and residual stresses, *Journal of Constructional Steel Research*. 47 (1998), pp. 193-210.

[34] Pham, C.: Direct Strength Method of Design of Cold-Formed Sections in shear, and Combined bending and shear, Ph.D, The University of Sydney, 2010.

[35] Schafer, B., Li, Z., Moen, C.: Computational modelling of cold-formed steel, *Thin-Walled Structures*, 48 (2010), pp. 752-762.

[36] Siahaan, R., Keerthan, P., Mahendran, M.: Finite element modeling of rivet fastened rectangular hollow flange channel beams subject to local buckling, *Engineering Structures*, 126 (2016), pp. 311-327.

[37] Keerthan, P., Mahendran, M.: Numerical modelling and design of lipped channel beams subject to shear, in: *7Th European Conference on Steel and Composite Structures*, 2014.

[38] Pham, C., Davis, A., Emmett, B.: Numerical investigation of cold-formed lapped Z purlins under combined bending and shear, *Journal Of Constructional Steel Research*, 95 (2014), pp. 116-125.

[39] Pham, C., Hancock, G., Numerical investigation of longitudinally stiffened web channels predominantly in shear, *Thin-Walled Structures*. 86 (2015), pp. 47-55.

[40] Sundararajah, L., Mahendran, M., Keerthan, P.: New design rules for lipped channel beams subject to web crippling under two-flange load cases, *Thin-Walled Structures*. 119 (2017), pp. 421-437.

[41] Sundararajah, L., Mahendran, M., Keerthan, P.: Experimental Studies of Lipped Channel Beams Subject to Web Crippling under Two-Flange Load Cases, *Journal Of Structural Engineering*. 142 (2016).

[42] Keerthan, P., Mahendran, M.: Experimental investigation and design of lipped channel beams in shear, Thin-Walled Structures. 86 (2015), pp. 174-184.

[43] Lian, Y., Uzzaman, A., Lim, J., Abdelal, G., Nash, D., Young, B.: Web crippling behaviour of cold-formed steel channel sections with web holes subjected to interior-one-flange loading condition-Part I: Experimental and numerical investigation, *Thin-Walled Structures*, 111 (2017), pp. 103-112.

[44] Lian, Y., Uzzaman, A., Lim, J., Abdelal, G., Nash, D., Young, B.: Web crippling behaviour of cold-formed steel channel sections with web holes subjected to interior-one-flange loading condition – Part II: parametric study and proposed design equations, *Thin-Walled Structures*, 114 (2017), pp. 92-106.

[45] Lian, Y., Uzzaman, A., Lim, J., Abdelal, G., Nash, D., Young, B.: Effect of web holes on web crippling strength of cold-formed steel channel sections under end-one-flange loading condition – Part I: Tests and finite element analysis, *Thin-Walled Structures*, 107 (2016), pp. 443-452.

[46] Lian, Y., Uzzaman, A., Lim, J., Abdelal, G., Nash, D., Young, B.:, Effect of web holes on web crippling strength of cold-formed steel channel sections under end-one-flange loading condition - Part II: Parametric study and proposed design equations, *Thin-Walled Structures*, 107 (2016), pp. 489-501.

[47] Uzzaman, A., Lim, J., Nash, D., Rhodes, J., Young, B.: Effect of offset web holes on web crippling strength of cold-formed steel channel sections under end-two-flange loading condition, *Thin-Walled Structures*, 65 (2013), pp. 34-48.

[48] Uzzaman, A., Lim, J., Nash, D., Rhodes, J., Young, B.: Web crippling behaviour of cold-formed steel channel sections with offset web holes subjected to interior-two-flange loading, *Thin-Walled Structures*, 50 (2012), pp. 76-86.

[49] Uzzaman, A., Lim, J., Nash, D., Rhodes, J., Young, B.: Cold-formed steel sections with web openings subjected to web crippling under two-flange loading conditions—part I: Tests and finite element analysis, *Thin-Walled Structures*, 56 (2012), pp. 38-48.

[50] Uzzaman, A., Lim, J., Nash, D., Rhodes, J., Young, B.: Cold-formed steel sections with web openings subjected to web crippling under two-flange loading conditions—Part II: Parametric study and proposed design equations, *Thin-Walled Structures*, 56 (2012), pp. 79-87.

Keywords: Cold-formed steel beams, Flexural capacity, Shear capacity, Web crippling capacity, Particle swarm optimization, Innovative sections, Finite element analyses

Authors

Perampalam Gatheeshgar
Northumbria University
Department of Mechanical and Construction Engineering
Newcastle upon Tyne, United Kingdom
g.perampalam@northumbria.ac.uk

Dr. Keerthan Poologanathan
Northumbria University
Department of Mechanical and Construction Engineering
Newcastle upon Tyne, United Kingdom
Keerthan.poologanathan@northumbria.ac.uk

Dr. Shanmuganathan Gunalan
Griffith University
School of Engineering and Built Environment
Gold Coast, Australia
s.gunalan@griffith.edu.au

Dr. Brabha Nagaratnam
Northumbria University
Department of Mechanical and Construction Engineering
Newcastle upon Tyne, United Kingdom
Brabha.Nagaratnam@northumbria.ac.uk

Dr. Konstantinos Daniel Tsavdaridis
University of Leeds
School of Civil Engineering
Leeds, United Kingdom
K.Tsavdaridis@leeds.ac.uk

Dr. Jun Ye
Imperial College London
Department of Civil and Environmental Engineering
London, United Kingdom
j.ye13@imperial.ac.uk

Table 1. Optimised dimensions and capacities of the selected sections

Prototypes	h (mm)	b (mm)	c (mm)	d (mm)	w_1 (mm)	w_2 (mm)	w_3 (mm)	δ_1 (°)	δ_2 (°)	M_{EC3} (kNm)	M_{FE} (kNm)	M_{FE} / M_{EC3}
Benchmark	231	75	17	-	-	-	-	-	-	10.30	10.41	1.01
Optimised-LCB	269	50	23	-	-	-	-	-	-	13.38	13.28	0.99
Folded-Flange	185	48	50	17	-	-	-	105	95	16.12	16.60	1.03
Super-Sigma	270	50	17.5	-	41	30	139	34	-	17.43	16.90	0.97
Mean												1.00
COV												0.026

Table 2. Validation of finite element results for bending with experiment results reported in [2]

LCB Specimens	h (mm)	b (mm)	c (mm)	r (mm)	t (mm)	fy (MPa)	Test [2] (kNm)	FE (kNm)	Test/ FE
Mw_C15015	152.70	64.77	16.57	5.00	1.50	514.10	9.5	9.6	0.99
Mw_C15019	153.38	64.47	16.00	5.00	1.90	534.50	12.9	13.6	0.95
Mw_C15024	152.60	62.70	19.70	5.00	2.40	485.30	17.7	16.6	1.08
Mw_C20015	203.70	76.08	16.42	5.00	1.50	513.40	12.2	13.3	0.92
Mw_C20019	202.60	77.92	17.28	5.00	1.90	510.50	18.9	21.3	0.89
Mw_C20024	202.35	76.61	20.38	5.00	2.40	483.50	27.8	27.6	1.01
Mean									0.97
COV									0.07

Note: r = inner radius, t = thickness, f_y = yield strength and others are defined in Figure 2(a)

Table 3. Validation of finite element results for shear with experiment results reported in [42]

LCB Specimens	a/d_1 (mm)	d1 (mm)	t (mm)	fy (MPa)	Test [34] (kN)	FE (kN)	Test/ FE
160×65×15×1.90	1.0	156.8	1.92	515	73.8	77.58	0.95
200×75×15×1.50	1.0	197.0	1.51	537	57.0	61.90	0.92
160×65×15×1.50	1.0	157.5	1.51	537	54.5	55.20	0.99
120×50×18×1.50	1.0	116.8	1.49	537	43.3	47.80	0.91
200×75×15×1.95	1.0	198.0	1.93	271	55.1	50.07	1.10
120×50×18×1.95.	1.0	118.6	1.95	271	38.1	34.88	1.10
Mean							0.99
COV							0.08

Note: a = shear span, d_1 = clear web height, t = thickness, f_y = yield strength

Table 4. Validation of finite element results for web crippling with experiment results reported in [41]

LCB Specimens	l_b (mm)	b (mm)	c (mm)	h (mm)	t (mm)	r (mm)	L (mm)	fy (MPa)	Test [33] (kN)	FE (kN)	Test/ FE
ITF-C10010	100	50.7	13.3	100.1	1.03	3.5	510	581	6.45	6.55	0.98
ITF-C10015	100	50.9	15.5	100.8	1.52	4.0	510	540	14.34	14.91	0.96
ITF-C15012	100	62.3	19.6	150.4	1.21	4.0	760	556	8.14	7.95	1.02
ITF-C15015	100	62.7	18.3	150	1.52	4.5	760	531	12.92	13.07	0.99
ITF-C20019	100	77.3	19.4	203.1	1.91	5.0	1015	506	20.19	19.93	1.01
ITF-C20024	100	76.7	20.2	203.6	2.41	5.0	1013	526	33.68	34.38	0.98
Mean											0.99
COV											0.02

Note: l_b = bearing plate length, t = thickness, r = inner radius, L = specimen length, f_y = yield strength and others are defined in Figure 2(a)

Table 5. Summary of the FE results for bending, shear and web crippling capacities for considered CFS sections

Prototypes	Bending	Shear	Web crippling
Benchmark 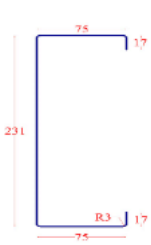	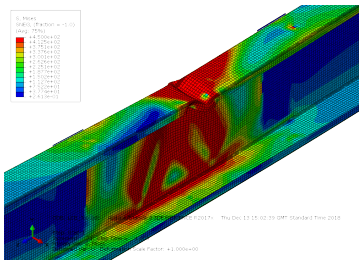 10.41 kNm (100%)	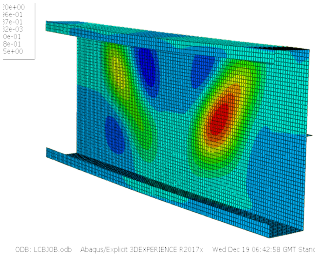 53.70 kN (100%)	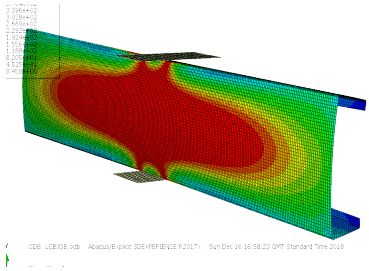 11.12 kN (100%)
Optimised-LCB 	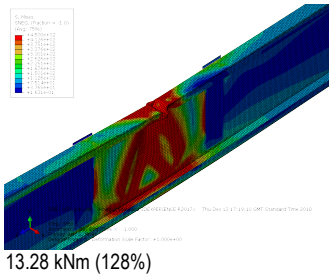 13.28 kNm (128%)	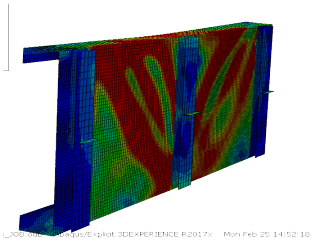 54.32 kN (101%)	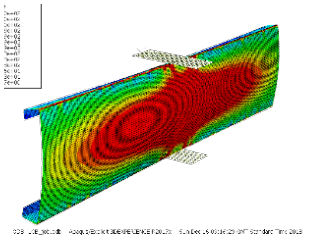 9.76 kN (88%)
Folded-Flange 	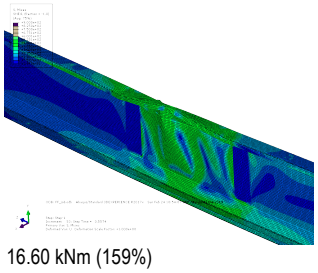 16.60 kNm (159%)	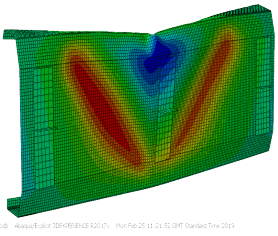 39.75 kN (74%)	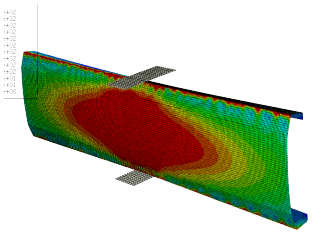 6.35 kN (57%)
Super-Sigma 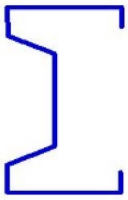	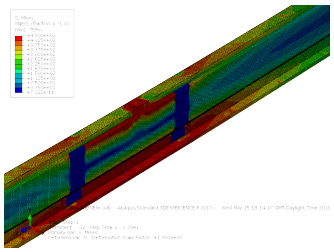 16.90 kNm (163%)	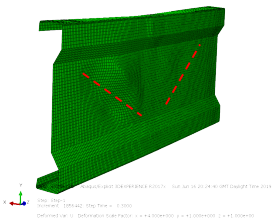 62.08 kN (116%)	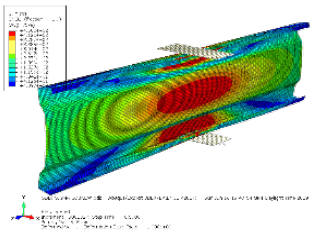 9.21 kN (83%)

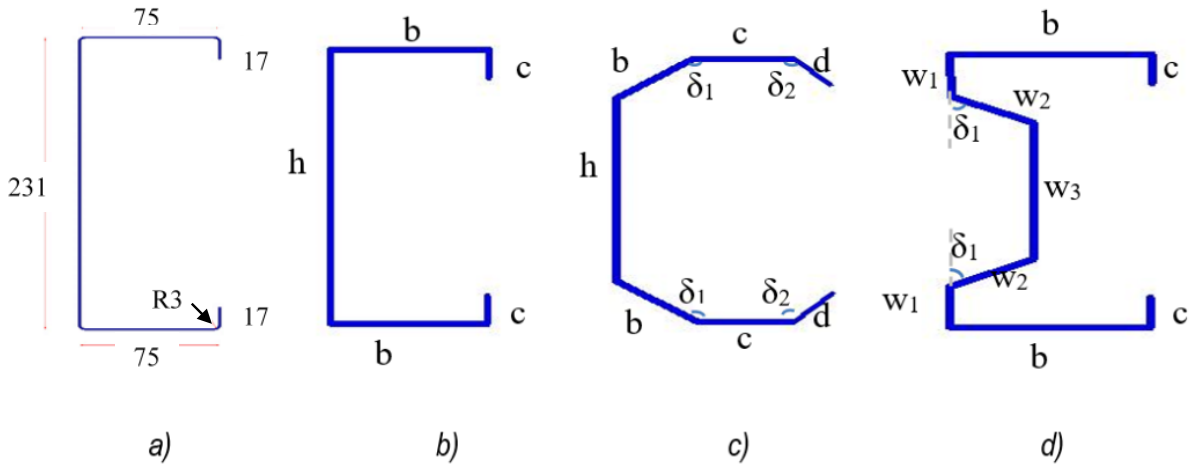

Fig. 1. *Selected CFS sections for investigation: (a) Benchmark; (b) Optimised LCB; (c) Folded-Flange; (d) Super-Sigma*

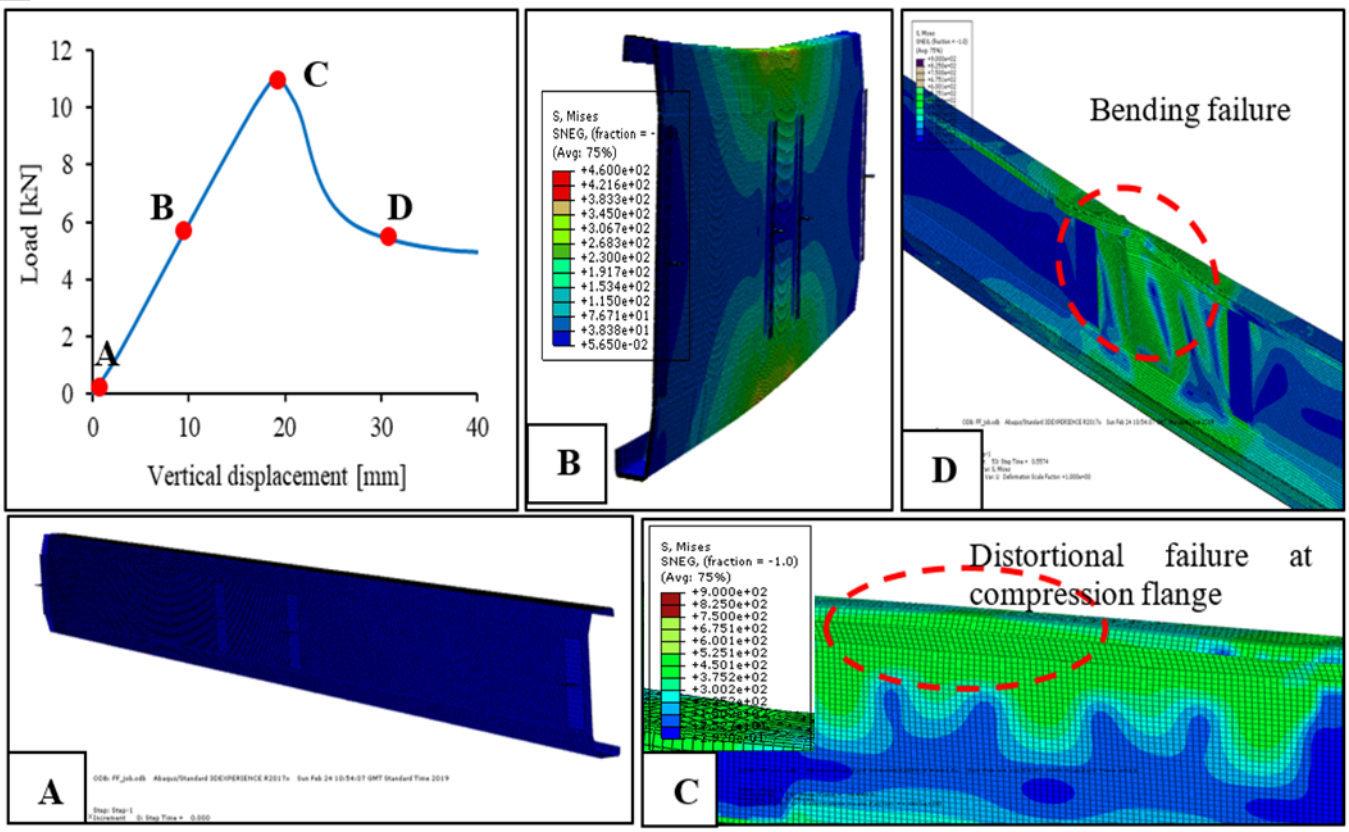

Fig. 2. *Failure modes (stress pattern) of Folded-Flange section subject to bending at different stages*

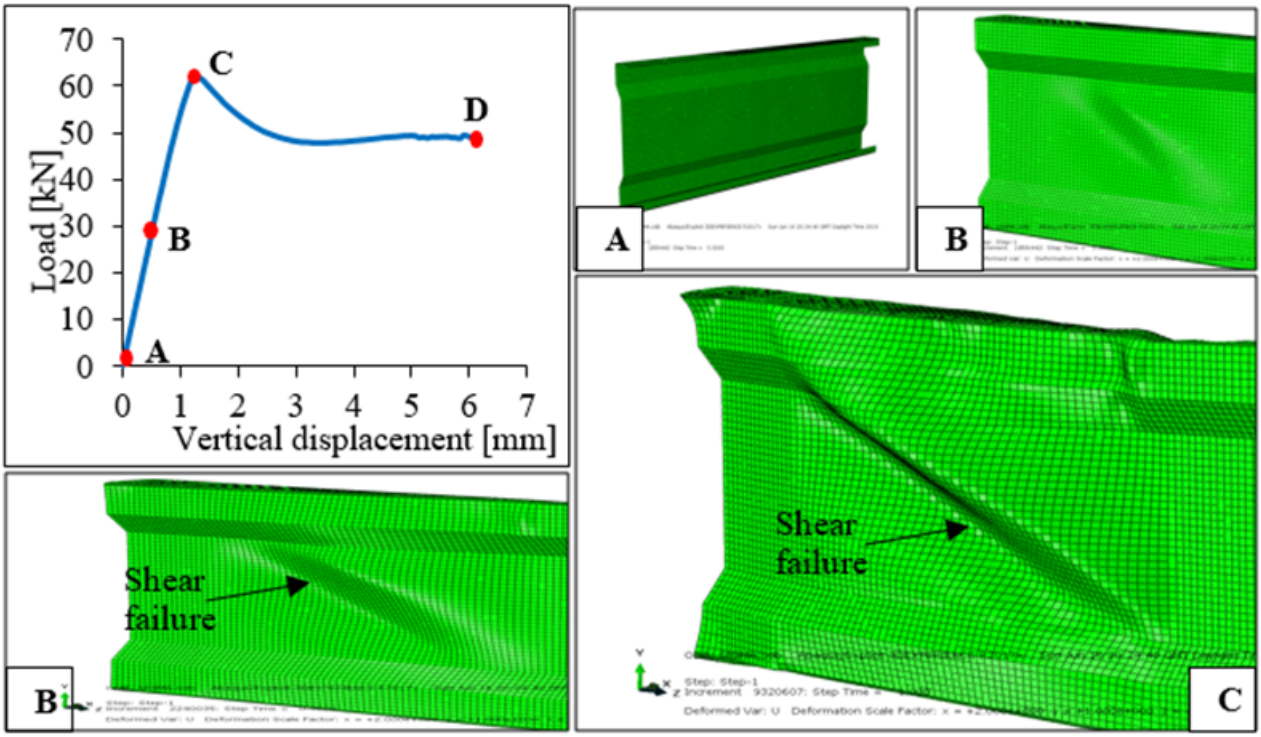

Fig. 3. *Failure modes (deformation pattern) of Super-Sigma section subject to shear at different stages*

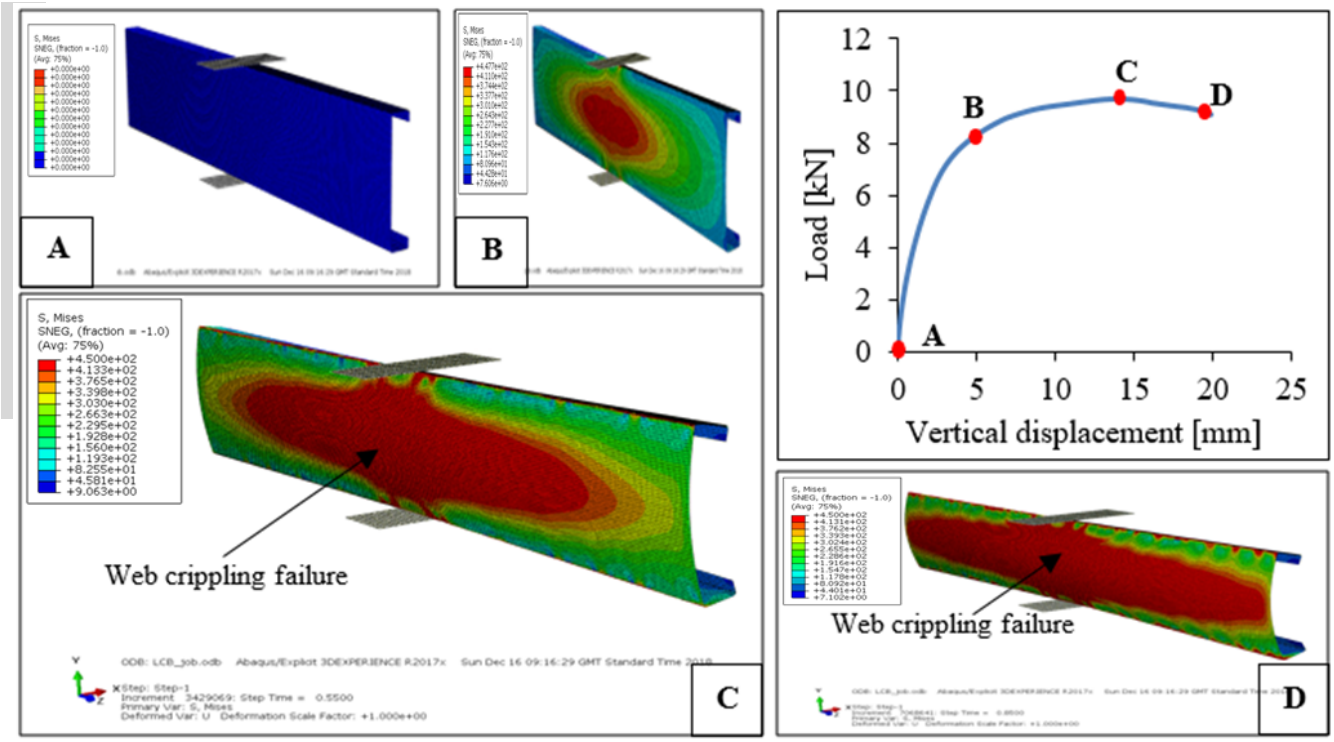

Fig. 4. *Failure modes (stress pattern) of Optimised LCB section subject to web crippling at different stages*

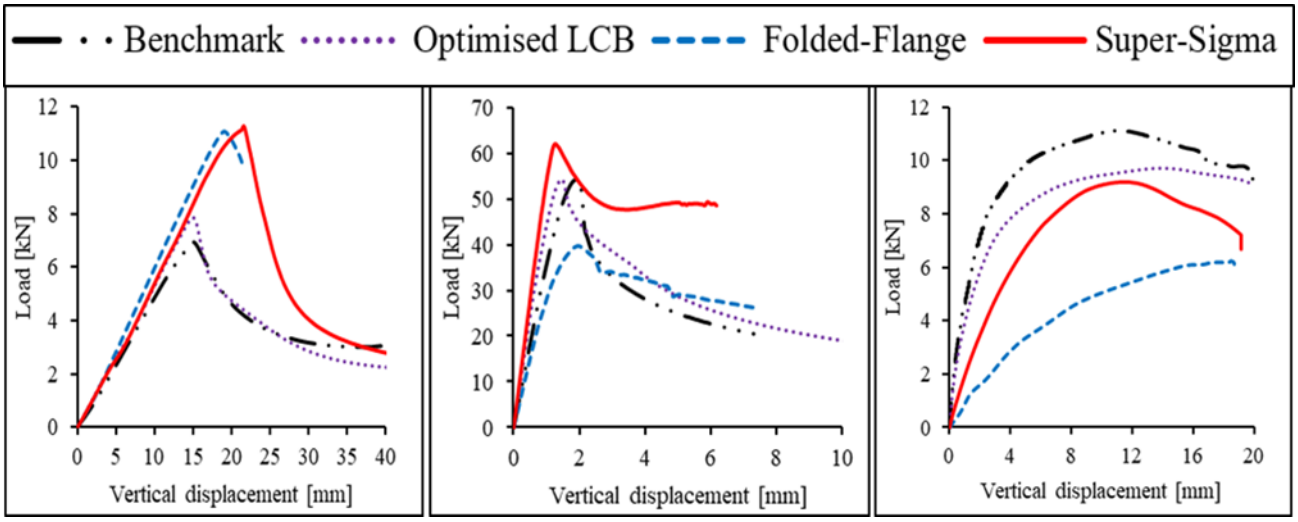

Fig. 5. *Load-displacement behaviour of all considered CFS obtained for (a) bending; (b) shear; and (c) web crippling actions*

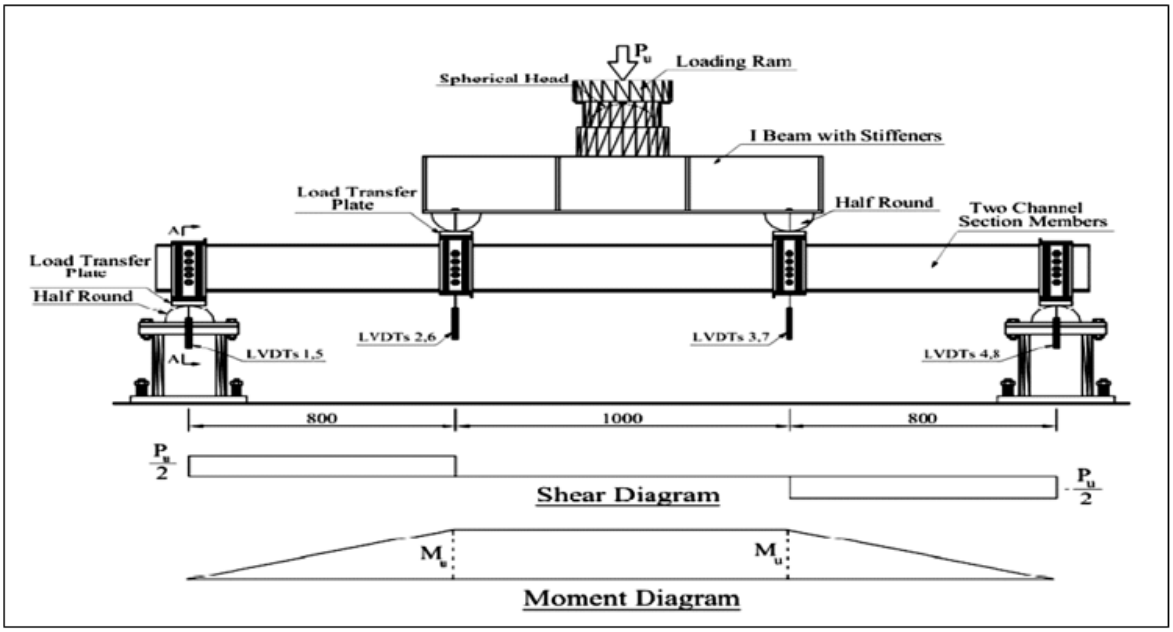

a)

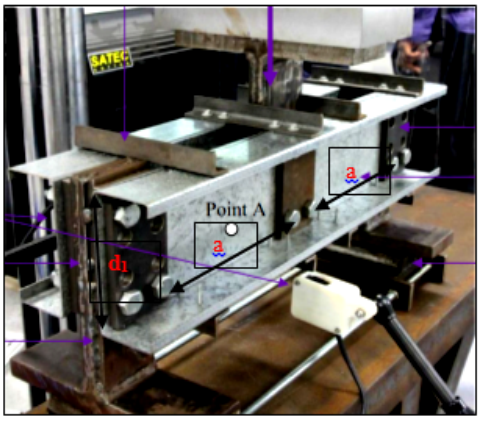

b)

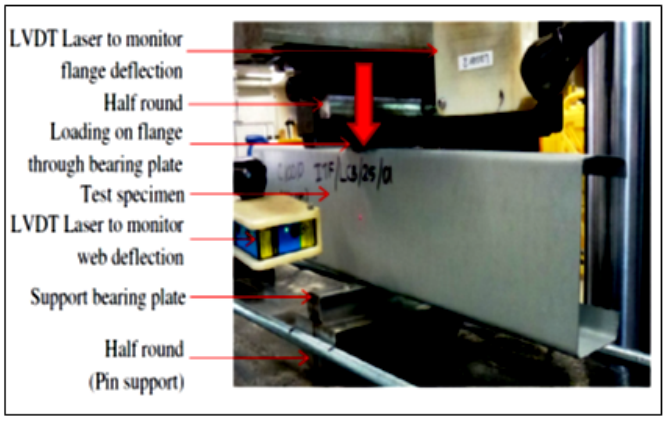

c)

Fig. 6. *Test arrangements considered for validation: (a) Bending [2]; (b) Shear [42]; (c) Web crippling [41]*

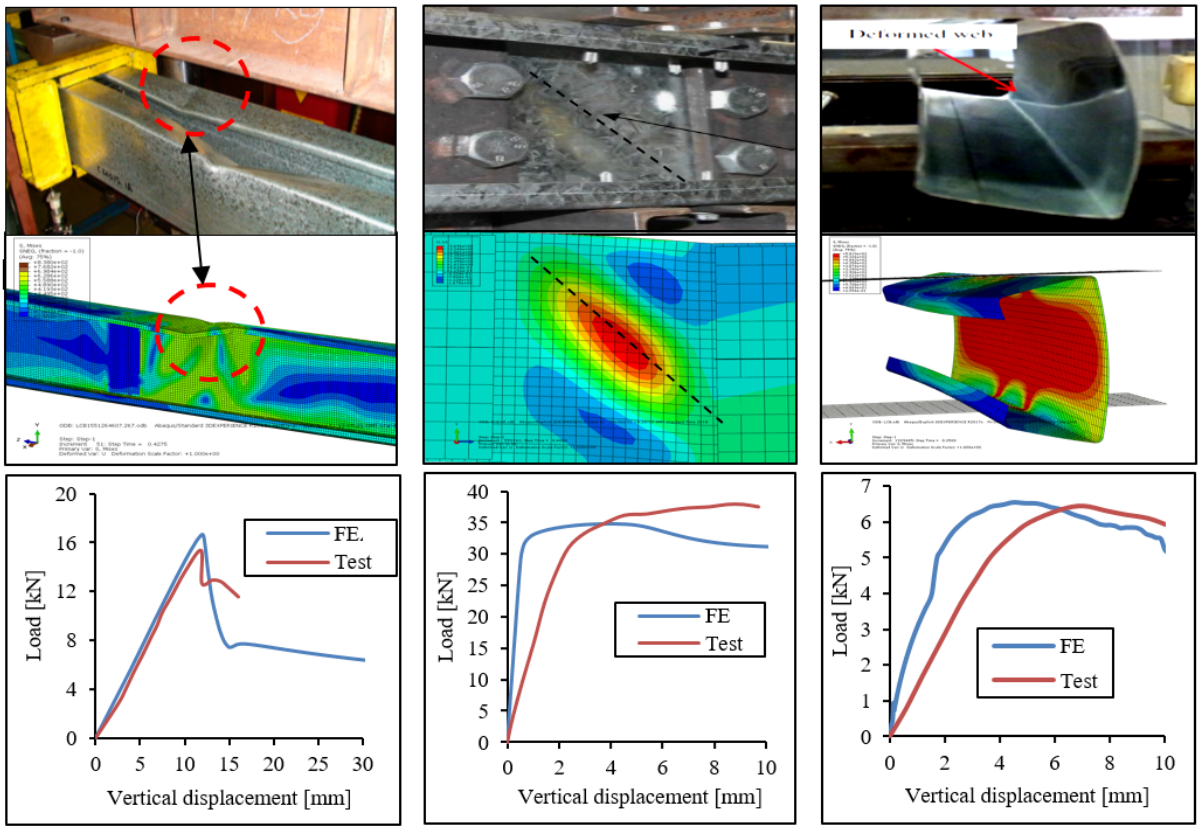

Fig. 7. *Comparison of FE failure modes and load-displacement behaviour with test results: (a) Bending [2]; (b) Shear [42]; (c) Web crippling [41]*